

## **ELECTROSTATIC DISCHARGE CURRENTS REPRESENTATION USING THE ANALYTICALLY EXTENDED FUNCTION WITH P PEAKS BY INTERPOLATION ON A D-OPTIMAL DESIGN**

**Karl Lundengård<sup>1</sup>, Milica Rančić<sup>1</sup>, Vesna Javor<sup>2</sup>, Sergei Silvestrov<sup>1</sup>**

<sup>1</sup>Division of Applied Mathematics, UKK, Mälardalen University, Västerås, Sweden

<sup>2</sup>Department of Power Engineering, Faculty of Electronic Engineering, University of Niš,  
Niš, Serbia

**Abstract.** *In this paper the Analytically Extended Function (AEF) with  $p$  peaks is used for representation of the electrostatic discharge (ESD) currents and lightning discharge currents. The fitting to data is achieved by interpolation of certain data points. In order to minimize unstable behaviour, the exponents of the AEF are chosen from a certain arithmetic sequence and the interpolated points are chosen according to a  $D$ -optimal design. The method is illustrated using several examples of currents taken from standards and measurements.*

**Key words:** *Analytically extended function, electrostatic discharge (ESD) current, lightning discharge current,  $D$ -optimal design.*

### 1 INTRODUCTION

Well-defined representation of real electrostatic discharge (ESD) currents is needed in order to establish realistic requirements for ESD generators used in testing of the equipment and devices, as well as to provide and improve the repeatability of tests. Such representations should be able to approximate the ESD currents waveshapes for various test levels, test set-ups and procedures, and also for various ESD conditions such as approach speeds, types of electrodes, relative arc length, humidity, etc. A mathematical function is needed for computer simulation of ESD phenomena, for verification of test generators and for improving standard waveshape definition.

---

Received December 21, 2018

**Corresponding author:** Karl Lundengård

Division of Applied Mathematics, UKK, Mälardalen University, Högscoleplan 1, Box 883, 721 23 Västerås, Sweden  
(E-mail: [karl.lundengard@mdh.se](mailto:karl.lundengard@mdh.se))

Functions previously proposed in the literature for modelling of ESD currents, are mostly linear combinations of exponential functions, Gaussian functions, Heidler functions or other functions, for a short review see for example [1]. The Analytically Extended Function (AEF) was initially proposed in [2] and has been successfully applied to lightning discharge modelling [3–13] using nonlinear least-square curve fitting.

In this paper we analyse the applicability of the AEF with  $p$  peaks to representation of ESD currents by interpolation of data points chosen according to a  $D$ -optimal design. This is illustrated through examples from two applications. The first application is modelling of an ESD commonly used in electrostatic discharge immunity testing, and the second modelling of lightning discharges.

For the ESD immunity testing application we model the IEC Standard 61000-4-2 waveshape, [14, 15] and an experimentally measured ESD current from [16].

For the lightning discharge application we model the IEC 61312-1 standard waveshape [17, 18] and a more complex measured lightning discharge current from [19]. We also use the same method to approximate a measured derivative of a lightning discharge current derivative from [20].

In both applications the basic properties of the current (or current derivative) are the same, these properties and how they are modelled with the AEF is discussed in the next section.

## 2 MODELLING OF ESD CURRENTS USING THE AEF

Various mathematical expressions have been introduced in the literature that can be used for representation of the ESD currents, either the IEC 61000-4-2 Standard one [15], or experimentally measured ones, e.g. [21]. These functions are to certain extent in accordance with the requirements given in Table 1. Furthermore, they have to satisfy the following:

- the value of the ESD current and its first derivative must be equal to zero at the moment  $t = 0$ , since neither the transient current nor the radiated field generated by the ESD current can change abruptly at that moment.
- the ESD current function must be time-integrable in order to allow numerical calculation of the ESD radiated fields.

## 2.1 The Analytically Extended Function (AEF) with $p$ peaks

A so-called analytically extended function (AEF) with  $p$  peaks has been proposed and applied by the authors to lightning discharge current modelling in [9–11]. Initial considerations on applying the function to ESD currents have also been made in [1, 5].

The AEF consists of scaled and translated functions of the form  $x(\beta; t) = (te^{1-t})^\beta$  that the authors have previously referred to as power-exponential functions [10].

Here we define the AEF with  $p$  peaks as

$$i(t) = \sum_{k=1}^{q-1} I_{m_k} + I_{m_q} \sum_{k=1}^{n_q} \eta_{q,k} x_{q,k}(t), \quad (1)$$

for  $t_{m_{q-1}} \leq t \leq t_{m_q}$ ,  $1 \leq q \leq p$ , and

$$\sum_{k=1}^p I_{m_k} \sum_{k=1}^{n_{p+1}} \eta_{p+1,k} x_{p+1,k}(t), \quad (2)$$

for  $t_{m_p} \leq t$ .

The current value of the first peak is denoted by  $I_{m_1}$ , the difference between each pair of subsequent peaks by  $I_{m_2}, I_{m_3}, \dots, I_{m_p}$ , and their corresponding times by  $t_{m_1}, t_{m_2}, \dots, t_{m_p}$ . In each time interval  $q$ , with  $1 \leq q \leq p+1$ , the number of terms is given by  $n_q$ ,  $0 < n_q \in \mathbb{Z}$ . Parameters  $\eta_{q,k}$  are such that  $\eta_{q,k} \in \mathbb{R}$  for  $q = 1, 2, \dots, p+1$ ,  $k = 1, 2, \dots, n_q$  and  $\sum_{k=1}^{n_q} \eta_{q,k} = 1$ .

Furthermore  $x_{q,k}(t)$ ,  $1 \leq q \leq p+1$  is given by

$$x_{q,k}(t) = \begin{cases} x\left(\beta_{q,k}; \frac{t-t_{m_{q-1}}}{t_{m_q}-t_{m_{q-1}}}\right), & 1 \leq q \leq p, \\ x\left(\beta_{q,k}; \frac{t}{t_{m_q}}\right), & q = p+1. \end{cases} \quad (3)$$

*Remark 1.* When previously applying the AEF, see [9–11], all exponents ( $\beta$ -parameters) of the AEF were set to  $\beta^2 + 1$  in order to guarantee that the derivative of the AEF is continuous. Here this condition will be satisfied in a different manner.

Since the AEF is a linear combination of elementary functions, its derivative and integral can be found using standard methods. Explicit formulae are given in [11, Theorems 1-3].

Previously, the authors have fitted AEF functions to lightning discharge currents and ESD currents using the Marquardt least square method but have noticed that the obtained result varies greatly depending on how the waveforms are sampled. This is problematic, especially since the methodology becomes computationally demanding when applied to large amounts of data. Here we will try one way to minimize the data needed but still enough to get as good approximation as possible.

The method examined here will be based on  $D$ -optimality of a regression model. A  $D$ -optimal design is found by choosing sample points such that the determinant of the Fischer information matrix of the model is maximized. For a standard linear regression model this is also equivalent, by the so-called Kiefer-Wolfowitz equivalence criterion, to  $G$ -optimality which means that the maximum of the prediction variance will be minimized. These are standard results in the theory of optimal design and a summary can be found for example in [22].

Minimizing the prediction variance will in our case mean maximizing the robustness of the model. This does not guarantee a good approximation but it will increase the chances of the method working well when working with limited precision and noisy data, and thus improve the chances of finding a good approximation when it is possible.

### 3 $D$ -OPTIMAL APPROXIMATION FOR EXPONENTS GIVEN BY A CLASS OF ARITHMETIC SEQUENCES

It can be desirable to minimize the number of points used when constructing the approximation. One way of doing this is choosing the  $D$ -optimal sampling points.

In this section we will only consider the case where in each interval the  $n$  exponents,  $\beta_1, \dots, \beta_n$ , are chosen according to

$$\beta_m = \frac{k + m - 1}{c}, \quad m = 1, 2, \dots, n$$

where  $k$  is a non-negative integer and  $c$  a positive real number. Note that in order to guarantee continuity of the AEF derivative the condition  $k > c$  has to be satisfied.

In each interval we want an approximation of the form

$$y(t) = \sum_{i=1}^n \eta_i t^{\beta_i} e^{\beta_i(1-t)}$$

and by setting  $z(t) = (te^{1-t})^{\frac{1}{c}}$  we obtain

$$y(t) = \sum_{i=1}^n \eta_i z(t)^{k+i-1}.$$

If we have  $n$  sample points,  $t_i$ ,  $i = 1, \dots, n$ , then the Fischer information matrix,  $M$ , of this system is  $M = U^T U$  where

$$U = \begin{bmatrix} z(t_1)^k & z(t_2)^k & \dots & z(t_n)^k \\ z(t_1)^{k+1} & z(t_2)^{k+1} & \dots & z(t_n)^{k+1} \\ \vdots & \vdots & \ddots & \vdots \\ z(t_1)^{k+n-1} & z(t_2)^{k+n-1} & \dots & z(t_n)^{k+n-1} \end{bmatrix}.$$

Thus if we want to maximize  $\det(M) = \det(U)^2$  it is sufficient to maximize or minimize the determinant  $\det(U)$ . Set  $z(t_i) = (t_i e^{1-t_i})^{\frac{1}{c}} = x_i$  then

$$\begin{aligned} u_n(t_1, \dots, t_n) &= \det(U) \\ &= \left( \prod_{i=1}^n x_i^k \right) \left( \prod_{1 \leq i < j \leq n} (x_j - x_i) \right). \end{aligned} \quad (4)$$

To find  $t_i$  we will use the Lambert  $W$  function. Formally the Lambert  $W$  function is the function  $W$  that satisfies  $t = W(te^t)$ . Using  $W$  we can invert  $z(t)$  in the following way

$$\begin{aligned} te^{1-t} = x^c &\Leftrightarrow -te^{-t} = -e^{-1}x^c \\ &\Leftrightarrow t = -W(-e^{-1}x^c). \end{aligned} \quad (5)$$

The Lambert  $W$  is multivalued but since we are only interested in real-valued solutions we are restricted to the main branches  $W_0$  and  $W_{-1}$ . Since  $W_0 \geq -1$  and  $W_{-1} \leq -1$  the two branches correspond to the rising and decaying parts of the AEF respectively. We will deal with the details of finding the correct points for the two parts separately.

### 3.1 $D$ -optimal interpolation on the rising part

Finding the  $D$ -optimal points on the rising part can be done using Theorem 1.

**Theorem 1.** *The determinant*

$$u_n(k; x_1, \dots, x_n) = \left( \prod_{i=1}^n x_i^k \right) \left( \prod_{1 \leq i < j \leq n} (x_j - x_i) \right)$$

where  $k \in \mathbb{R}$  is maximized or minimized on the cube  $[0, 1]^n$  when  $x_1 < \dots < x_{n-1}$  are roots of the Jacobi polynomial

$$P_{n-1}^{(2k-1, 0)}(1-2x) = \frac{(2k)^{\overline{n-1}}}{(n-1)!} \sum_{i=0}^{n-1} (-1)^n \binom{n-1}{i} \frac{(2k+n)^{\bar{i}}}{(2k)^{\bar{i}}} x^i$$

and  $x_n = 1$ , or some permutation thereof.

Here  $a^{\bar{b}}$  is the rising factorial  $a^{\bar{b}} = a(a+1) \cdots (a+b-1)$ .

*Proof.* Without loss of generality we can assume  $0 < x_1 < x_2 < \dots < x_{n-1} < x_n \leq 1$ . Fix all  $x_i$  except  $x_n$ . When  $x_n$  increases all factors of  $u_n$  that contain  $x_n$  will also increase, thus  $u_n$  will reach its maximum value on the edge of the cube where  $x_n = 1$ . Using the method of Lagrange multipliers in the plane given by  $x_n = 1$  gives

$$\frac{\partial u_n}{\partial x_j} = u_n(k; x_1, \dots, x_n) \left( \frac{k}{x_j} + \sum_{\substack{i=1 \\ i \neq j}}^n \frac{1}{x_j - x_i} \right) = 0,$$

for  $j = 1, \dots, n-1$ . By setting  $f(x) = \prod_{i=1}^n (x - x_i)$  we get

$$\begin{aligned} \frac{k}{x_j} + \sum_{\substack{i=1 \\ i \neq j}}^n \frac{1}{x_j - x_i} = 0 &\Leftrightarrow \frac{k}{x_j} + \frac{1}{2} \frac{f''(x_j)}{f'(x_j)} = 0 \\ &\Leftrightarrow x_j f''(x_j) + 2k f'(x_j) = 0 \end{aligned} \quad (6)$$

for  $j = 1, \dots, n-1$ . Since  $f(x)$  is a polynomial of degree  $n$  that has  $x = 1$  as a root then equation (6) implies

$$x f''(x) + 2k f'(x) = c \frac{f(x)}{x-1}$$

where  $c$  is some constant. Set  $f(x) = (x-1)g(x)$  and the resulting differential equation is

$$x(x-1)g''(x) + ((2k+2)x-2k)g'(x) + (2k-c)g(x) = 0.$$

The constant  $c$  can be found by examining the terms with degree  $n-1$  and is given by  $c = 2k + (n-1)(2k+n)$ , thus

$$\begin{aligned} x(1-x)g''(x) + (2k - (2k+2)x)g'(x) \\ + (n-1)(2k+n)g(x) = 0. \end{aligned} \quad (7)$$

Comparing (7) with the standard form of the hypergeometric function [23]

$$x(1-x)g''(x) + (c - (a+b+1)x)g'(x) - abg(x) = 0$$

shows that  $g(x)$  can be expressed as follows

$$\begin{aligned} g(x) &= C \cdot {}_2F_1(1-n, 2k+n; 2k, x) \\ &= C \cdot \frac{(2k)^{\overline{n-1}}}{(n-1)!} \sum_{i=0}^{n-1} (-1)^i \binom{n-1}{i} \frac{(2k+n)^{\overline{i}}}{(2k)^{\overline{i}}} x^i \end{aligned}$$

where  $C$  is an arbitrary constant and since we are only interested in the roots of the polynomial we can choose  $C$  so that it gives the desired form of the expression. The connection to the Jacobi polynomial is given by [23]

$${}_2F_1(-m, 1+\alpha+\beta+n; \alpha+1; x) = \frac{m!}{(\alpha+1)^{\overline{m}}} P_m^{(\alpha, \beta)}(1-2x),$$

and  $\alpha = 2k-1$ ,  $\beta = 0$ ,  $m = n-1$  gives the expression in Theorem 1. Note that the Jacobi polynomials  $P_n^{(a,b)}(x)$  are orthogonal polynomials on the interval  $[-1, 1]$  with respect to the weight function  $(1-x)^a(1+x)^b$  and thus all of its zeros will be real, distinct and located in  $[-1, 1]$ , see [24]. Thus all zeros of the polynomial given in Theorem 1 will be real, distinct and located in the interval  $[0, 1]$ .  $\square$

We can now find the  $D$ -optimal  $t$ -values using the upper branch of the Lambert W function as described in equation (5),

$$t_i = -W_0(-e^{-1}x_i^c),$$

where  $x_i$  are the roots of the Jacobi polynomial given in Theorem 1. Since  $-1 \leq W_0(x) \leq 0$  for  $-e^{-1} \leq x \leq 0$  this will always give  $0 \leq t_i \leq 1$ .

*Remark 2.* Note that  $x_n = 1$  means that  $t_n = t_q$  and also is equivalent to

the condition  $\sum_{r=1}^{n_q} \eta_{q,r} = 1$ . In other words, we are interpolating the peak and  $p-1$  points inside each interval.

### 3.2 $D$ -optimal interpolation on the decaying part

Finding the  $D$ -optimal points for the decaying part is more difficult than it is for the rising part. Suppose we denote the largest value for time that can reasonably be used (for computational or experimental reasons) with  $t_{max}$ . This corresponds to some value  $x_{max} = (t_{max} \exp(1 - t_{max}))^{\frac{1}{c}}$ . Ideally we would want a corresponding theorem to Theorem 1 over  $[1, x_{max}]^n$  instead of  $[0, 1]^n$ . It is easy to see that if  $x_i = 0$  or  $x_i = 1$  for some  $1 \leq x_i \leq n - 1$  then  $w_n(k; x_1, \dots, x_n) = 0$  and thus there must exist some local extreme point such that  $0 < x_1 < x_2 < \dots < x_{n-1} < 1$ . This is no longer guaranteed when considering the volume  $[1, x_{max}]^n$  instead. Therefore we will instead extend Theorem 1 to the volume  $[0, x_{max}]^n$  and give an extra constraint on the parameter  $k$  that guarantees  $1 < x_1 < x_2 < \dots < x_{n-1} < x_n = x_{max}$ .

**Theorem 2.** *Let  $y_1 < y_2 < \dots < y_{n-1}$  be the roots of the Jacobi polynomial  $P_{n-1}^{(2k-1,0)}(1-2y)$ . If  $k$  is chosen such that  $1 < x_{max} \cdot y_1$  then the determinant  $w_n(k; x_1, \dots, x_n)$  given in Theorem 1 is maximized or minimized on the cube  $[1, x_{max}]^n$  (where  $x_{max} > 1$ ) when  $x_i = x_{max} \cdot y_i$  and  $x_n = x_{max}$ , or some permutation thereof.*

*Proof.* This theorem follows from Theorem 1 combined with the fact that  $w_n(k; x_1, \dots, x_n)$  is a homogeneous polynomial. Since  $w_n(k; b \cdot x_1, \dots, c \cdot x_n) = b^{k + \frac{n(n-1)}{2}} \cdot w_n(k; x_1, \dots, x_n)$  if  $(x_1, \dots, x_n)$  is an extreme point in  $[0, 1]^n$  then  $(b \cdot x_1, \dots, b \cdot x_n)$  is an extreme point in  $[0, b]^n$ . Thus by Theorem 1 the points given by  $x_i = x_{max} \cdot y_i$  will maximize or minimize  $w_n(k; x_1, \dots, x_n)$  on  $[0, x_{max}]^n$ .  $\square$

*Remark 3.* It is in many cases possible to ensure the condition  $1 < x_{max} \cdot y_1$  without actually calculating the roots of  $P_{n-1}^{(2k-1,0)}(1-2y)$ . In the literature on orthogonal polynomials there are many expressions for upper and lower bounds of the roots of the Jacobi polynomials. For instance in [25] an upper bound on the largest root of a Jacobi polynomial is given and can be, in our case, rewritten as

$$y_1 > 1 - \frac{3}{4k^2 + 2kn + n^2 - k - 2n + 1}$$

and thus

$$1 - \frac{3}{4k^2 + 2kn + n^2 - k - 2n + 1} > \frac{1}{x_{max}}$$

guarantees that  $1 < x_{max} \cdot y_1$ . If a more precise condition is needed there are expressions that give tighter bounds of the largest root of the Jacobi polynomials, see [26].

We can now find the  $D$ -optimal  $t$ -values using the lower branch of the Lambert  $W$  function as in equation (5),

$$t_i = -W_{-1}(-e^{-1}x_i^c),$$

where  $x_i$  are the roots of the Jacobi polynomial given in Theorem 1. Since  $-1 \leq W_{-1}(x) < -\infty$  for  $-e^{-1} \leq x \leq 0$  this will always give  $1 \leq t_i < t_{max} = -W_{-1}(-e^{-1}x_{max})$  so  $x_{max}$  is given by the highest feasible  $t$ .

*Remark 4.* Note that here just like in the rising part  $t_n = t_p$  which means that we will interpolate to the final peak as well as  $p-1$  points in the decaying part.

## 4 EXAMPLES OF MODELS FROM APPLICATIONS AND EXPERIMENTS

In this section some results of applying the described scheme to two different applications will be presented. The first application is modelling of ESD currents commonly used in electrostatic discharge immunity testing, and the second modelling of lightning discharge currents.

The values of  $n$  and peak-times have been chosen manually, and  $k$  and  $c$  have been chosen by first fixing  $k$  and then numerically finding a  $c$  that gave a close approximation. For this purpose we used software for numerical computing [27], based on the interior reflective Newton method described in [28, 29]. This is then repeated for  $k = 1, \dots, 10$  and the best fitting set of parameters is chosen. Note that this methodology uses all available data points to evaluate fitting but could probably be simplified further. For example, by using a simpler method for choosing  $c$  given  $k$ , only use a subset of available points to assess accuracy or, with sufficient experimentation find some suitable heuristic for choosing the appropriate value of  $k$ . Since the waveforms are given as data rather than explicit functions the  $D$ -optimal points have been calculated and then the closest available data points have been chosen.

In these examples we did not require that the coefficients in the linear sums were positive.

### 4.1 Modelling of ESD currents

#### 4.1.1 The IEC 61000-4-2 standard current waveshape

ESD generators used in testing of the equipment and devices should be able to reproduce the same ESD current waveshape each time. This repeata-

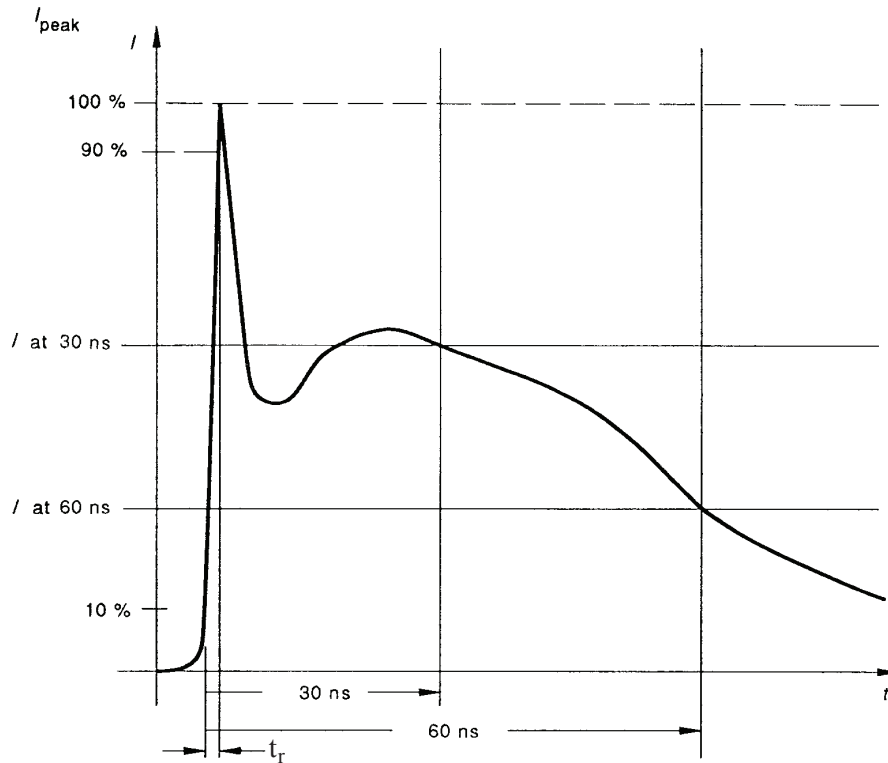


Fig. 1: Illustration of the IEC 61000-4-2 Standard ESD current and its key parameters, [15].

bility feature is ensured if the design is carried out in compliance with the requirements defined in the IEC 61000-4-2 Standard, [15].

Among other relevant issues, the Standard includes graphical representation of the typical ESD current, fig. 1, and also defines, for a given test level voltage, required values of ESD current's key parameters. These are listed in Table 1 for the case of the contact discharge, where:

- $I_{peak}$  is the ESD current initial peak;
- $t_r$  is the rising time defined as the difference between time moments corresponding to 10% and 90% of the current peak  $I_{peak}$ , fig. 1;
- $I_{30}$  and  $I_{60}$  are the ESD current values calculated for time periods of 30 and 60 ns, respectively, starting from the time point corresponding to 10% of  $I_{peak}$ , fig. 1.

**Table 1:** IEC 61000-4-2 standard ESD current and its key parameters, [15].

Voltage [kV]	$I_{peak}$ [A]	$t_r$ [ns]	$I_{30}$ [A]	$I_{60}$ [A]
2	$7.5 \pm 15\%$	$0.8 \pm 25\%$	$4.0 \pm 30\%$	$2.0 \pm 30\%$
4	$15.0 \pm 15\%$	$0.8 \pm 25\%$	$8.0 \pm 30\%$	$4.0 \pm 30\%$
6	$22.5 \pm 15\%$	$0.8 \pm 25\%$	$12.0 \pm 30\%$	$6.0 \pm 30\%$
8	$30.0 \pm 15\%$	$0.8 \pm 25\%$	$16.0 \pm 30\%$	$8.0 \pm 30\%$

In this section we present the results of fitting a 2-peak AEF to the Standard ESD current given in IEC 61000-4-2. Data points which are used in the optimization procedure are manually sampled from the graphically given Standard [15] current function, fig. 1. The peak currents and corresponding times are also extracted, and the results of  $D$ -optimal interpolation with two peaks are illustrated, see fig. 2. The parameters are listed in Table 3. In the illustrated examples a fairly good fit is found but typically areas with steeply rising and decaying parts are somewhat more difficult to fit with good accuracy than the other parts of the waveform.

#### 4.1.2 3-peaked AEF representing measured current from ESD

In this section we present the results of fitting a 3-peaked AEF to a waveform from experimental measurements from [16]. The result is also compared to a common type of function used for modelling ESD current, also from [16].

In figs. 3 and 4 the results of the interpolation of  $D$ -optimal points are shown together with the measured data, as well as a sum of two Heidler functions that was fitted to the experimental data in [16]. This function is given by

$$i(t) = I_1 \frac{\left(\frac{t}{\tau_1}\right)^{n_H}}{1 + \left(\frac{t}{\tau_1}\right)^{n_H}} e^{-\frac{t}{\tau_2}} + I_2 \frac{\left(\frac{t}{\tau_3}\right)^{n_H}}{1 + \left(\frac{t}{\tau_3}\right)^{n_H}} e^{-\frac{t}{\tau_4}},$$

$$I_1 = 31.365 \text{ A}, \quad I_2 = 6.854 \text{ A}, \quad n_H = 4.036,$$

$$\tau_1 = 1.226 \text{ ns}, \quad \tau_2 = 1.359 \text{ ns},$$

$$\tau_3 = 3.982 \text{ ns}, \quad \tau_4 = 28.817 \text{ ns}.$$

Note that this function does not reproduce the second local minimum but that all three AEF functions can reproduce all local minima and maxima

**Table 2:** IEC 61312-1 standard current waveshape and its key parameters, [17].

Protection level	Parameter	First stroke	Subsequent stroke
	$n$	10	10
	$T$	19.0 $\mu s$	0.454 $\mu s$
	$\tau$	485 $\mu s$	143 $\mu s$
	$\eta$	0.930	0.993
I	$I_{peak}$	200 kA	50 kA
II	$I_{peak}$	150 kA	37.5 kA
III-IV	$I_{peak}$	100 kA	25 kA

(to a modest degree of accuracy) when suitable values for the  $n$ ,  $k$  and  $c$  parameters are chosen. In fig. 4 we can see that even small bumps in the rising part are successfully reproduced.

## 4.2 Modelling of lightning discharge currents

### 4.2.1 IEC 61312-1 standard current waveshape

In this section we use the scheme to represent the IEC 61312-1 Standard current wave shape as it is described in [18]. Rather than being given graphically, as the IEC 61000-4-2 Standard current waveform, the shape is described using a Heidler function,

$$i(t) = \frac{I_{peak}}{\eta} \frac{\left(\frac{t}{T}\right)^n}{1 + \left(\frac{t}{T}\right)^n} e^{-\frac{t}{\tau}} \quad (8)$$

whose parameters are chosen according to Table 2.

In figs. 5 and 6 the results of fitting an AEF by interpolating on a  $D$ -optimal design to the first stroke of a protection level I IEC 61312-1 Standard waveshape are shown. The parameters of the fitted AEF are given in Table 5. In this case the waveshape can be reproduced fairly well but gives a relatively complicated expression compared to (8).

### 4.2.2 Modelling a measured lightning discharge current

In this section we fit an AEF function both with free parameters (as in [6]) and using interpolation on a  $D$ -optimal design, to data extracted from [20] that comes from measurements of a lightning strike on Mount Säntis in Switzerland [30].

We used a 13-peaked AEF and the results are shown in figs. 7a, 7c and 7e. Often the curves are similar enough that it can be hard to spot the differences so the residuals of the two models relative to the measured current is shown in figs. 7b, 7d and 7f. It can be seen that in most cases the AEF with free parameters gives a closer fit but the version interpolated on a  $D$ -optimal design is often comparable. Parameters for the  $D$ -optimal fitting can be found in Table 6.

### 4.2.3 Modelling the lightning discharge current derivative

Here we present some results when attempting to reproduce the derivative of the waveshape of the lightning discharge current using the AEF interpolated on a  $D$ -optimal design. We also compare the result of this fitting scheme to the results in [13] where the parameters of the AEF are chosen freely and fitted using the Marquardt Least-Squares Method.

The method for fitting an AEF described in this paper is applied to the modelling of lightning current derivative signals measured at the CN Tower [20]. The results of the fitting can be seen in fig. 8. From these figures it is clear that in this case of several peaks and few terms in each interval the two schemes for fitting the AEF are often similar in quality but sometimes the extra flexibility offered when letting all the exponents in the AEF be chosen individually can give a significantly better fit, an example of this can be seen in fig. 8. A possible explanation for this in this case is that in the scheme for  $D$ -optimal fitting you need many terms in order to have both small and large exponents. In fig. 9 we examine how well the different fitting schemes model the current when they are integrated. Here we can see that the free parameter version gives a considerably better matching to the numerically integrated measured values than the  $D$ -optimal fitting version.

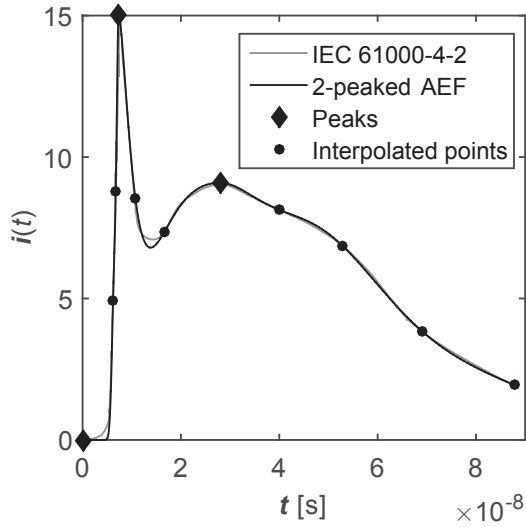


**Fig. 2:** 2-peaked AEF representing the IEC 61000-4-2 Standard ESD current waveshape for 4kV. Parameters are given in Table 3.

**Table 3:** Parameters' values of AEF with 2 peaks representing the IEC 61000-4-2 standard waveshape.

Local maxima and minima and corresponding times extracted from the IEC 61000-4-2, [15]			
$I_{max1} = 15$ [A]	$I_{min1} = 7.1484$ [A]	$I_{max2} = 9.0921$ [A]	
$t_{max1} = 6.89$ [ns]	$t_{min1} = 12.85$ [ns]	$t_{max2} = 25.54$ [ns]	
Parameters of interpolated AEF shown in fig. 2			
Interval	$n$	$k$	$c$
$0 \leq t \leq t_{max1}$	3	1	0.01385
$t_{max1} \leq t \leq t_{max2}$	3	4	2.025
$t_{max2} < t$	5	10	2.395

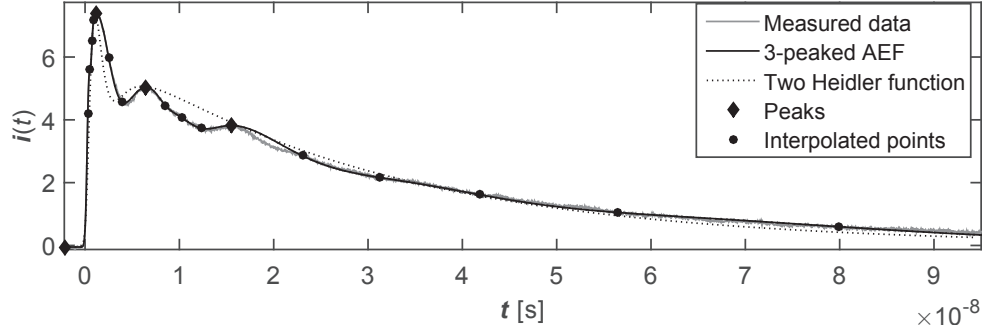


**Fig. 3:** 3-peaked AEF interpolated to  $D$ -optimal points chosen from measured ESD current from [16, fig.3] compared with the sum of two Heidler functions suggested in [16]. Parameters are given in Table 4.

**Table 4:** Parameters' values of AEF with 3 peaks representing measured ESD.

Local maxima and corresponding times extracted from [16, fig.3]			
$I_{max1} = 7.37$ [A]	$I_{max2} = 5.02$ [A]	$I_{max3} = 3.82$ [A]	
$t_{max1} = 1.23$ [ns]	$t_{max2} = 6.39$ [ns]	$t_{max3} = 15.5$ [ns]	
Parameters of interpolated AEF shown in fig. 3			
Interval	$n$	$k$	$c$
$0 \leq t \leq t_{max1}$	5	5	0.05750
$t_{max1} \leq t \leq t_{max2}$	3	1	0.4920
$t_{max2} \leq t \leq t_{max3}$	4	2	0.5967
$t_{max3} < t$	6	1	1.019

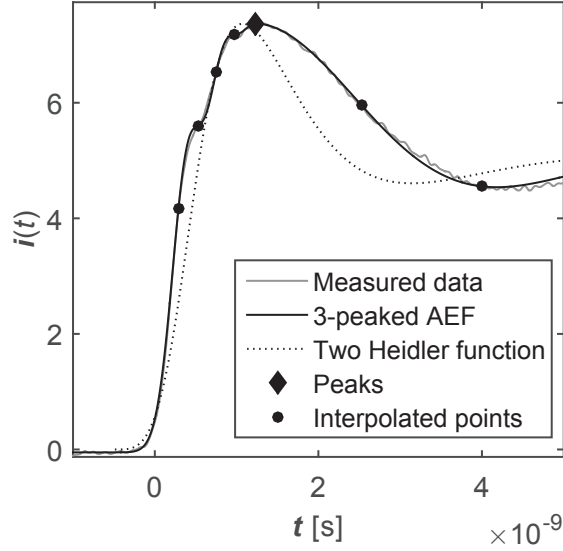


**Fig. 4:** Close-up of the rising part of a 3-peaked AEF interpolated to  $D$ -optimal points chosen from measured ESD current from [16, fig.3]. Parameters are given in Table 4.

**Table 5:** Parameters' values of AEF representing the IEC 61312-1 standard waveshape.

Chosen peak time and current			
$t_{max} = 28.14 [\mu s]$		$I = 92.54 [kA]$	
Parameters of interpolated AEF shown in fig. 5			
Interval	$n$	$k$	$c$
$0 \leq t \leq t_{max}$	4	10	0.7565
$t_{max} < t$	5	1	41.82

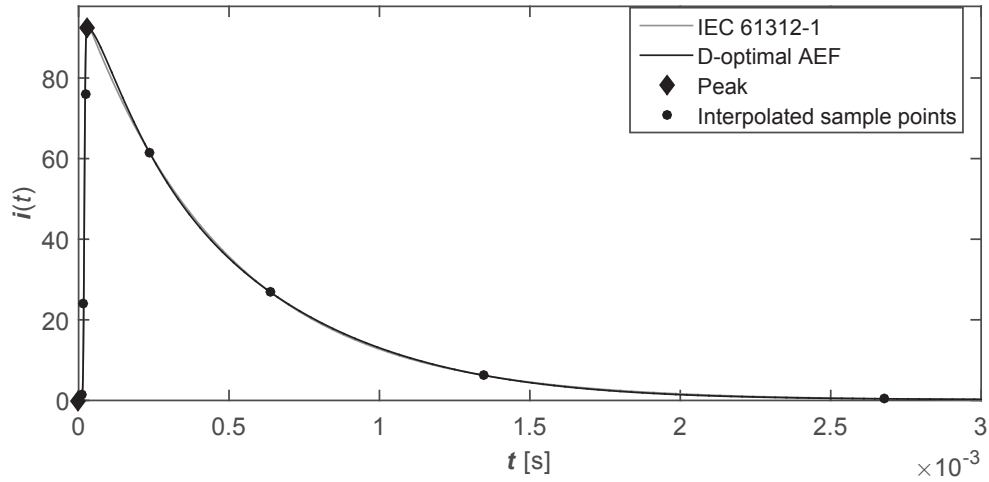


**Fig. 5:** AEF with 1 peak fitted by interpolating  $D$ -optimal points sampled from the Heidler function describing the IEC 61312-1 waveshape given by (8). Parameters are given in Table 5.

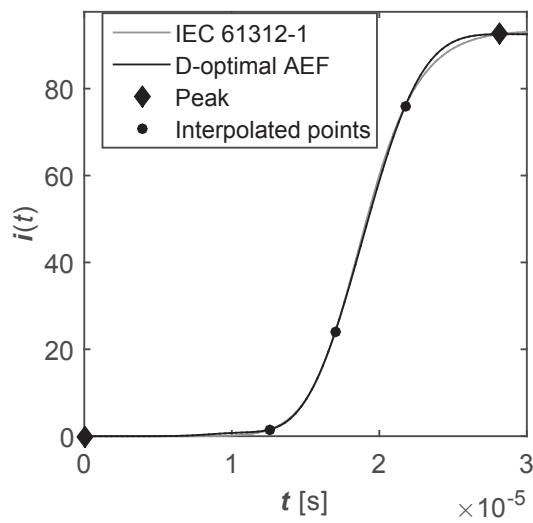


**Fig. 6:** Close-up of the rising part of the AEF with 1 peak fitted by interpolating  $D$ -optimal points samples from the Heidler function describing the IEC61312-1 waveshape given by (8). Parameters are given in Table 5.

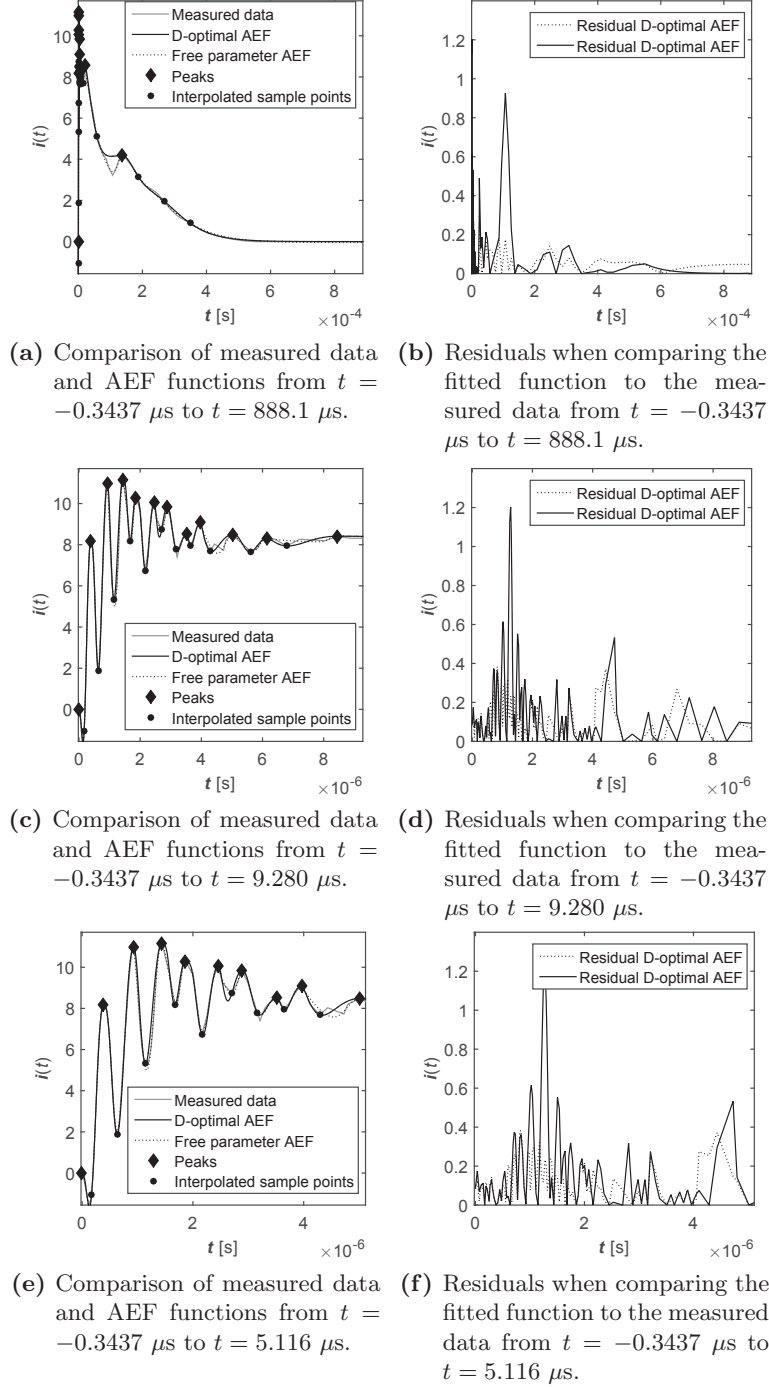


**Fig. 7:** Comparison of two AEFs with 13 peaks and 2 terms in each linear combination fitted to measured lightning discharge current derivative from [19]. One is fitted by interpolation on  $D$ -optimal points and the other is fitted with free parameters using the MLSM method. Parameters of the  $D$ -optimal version are given in Table 6.

**Table 6:** Parameters' values of AEF with 13 peaks representing measured data for a lightning discharge current from [30]. Local maxima and corresponding times extracted from [19, figs.6, 7 and 8] are denoted  $t$  and  $I$  and other parameters correspond to the fitted AEF shown in figs. 7a, 7c and 7e.

Peak times and currents		Parameters of fitted AEF			
$t$ [ $\mu\text{s}$ ]	$I$ [ $\mu\text{s}$ ]	Interval	$n$	$k$	$c$
$t_1 = 0.3998$	$I_1 = 8.159$	$0 \leq t \leq t_1$	2	2	0.4773
$t_2 = 0.9468$	$I_2 = 10.96$	$t_1 \leq t \leq t_2$	2	10	2.148
$t_3 = 1.458$	$I_3 = 11.14$	$t_2 \leq t \leq t_3$	2	1	0.3964
$t_4 = 1.873$	$I_4 = 10.26$	$t_3 \leq t \leq t_4$	2	1	0.2210
$t_5 = 2.475$	$I_5 = 10.07$	$t_4 \leq t \leq t_5$	2	10	1.695
$t_6 = 2.904$	$I_6 = 9.819$	$t_5 \leq t \leq t_6$	2	1	0.4591
$t_7 = 3.533$	$I_7 = 8.519$	$t_6 \leq t \leq t_7$	2	1	0.3503
$t_8 = 3.985$	$I_8 = 9.097$	$t_7 \leq t \leq t_8$	2	10	3.716
$t_9 = 5.036$	$I_9 = 8.485$	$t_8 \leq t \leq t_9$	2	1	0.6963
$t_{10} = 6.168$	$I_{10} = 8.310$	$t_9 \leq t \leq t_{10}$	2	1	0.2954
$t_{11} = 8.472$	$I_{11} = 8.413$	$t_{10} \leq t \leq t_{11}$	2	6	3.074
$t_{12} = 20.48$	$I_{12} = 8.576$	$t_{11} \leq t \leq t_{12}$	2	1	0.2784
$t_{13} = 137.5$	$I_{13} = 4.178$	$t_{12} \leq t \leq t_{13}$	2	1	0.6456
		$t_{13} < t$	4	1	0.3559

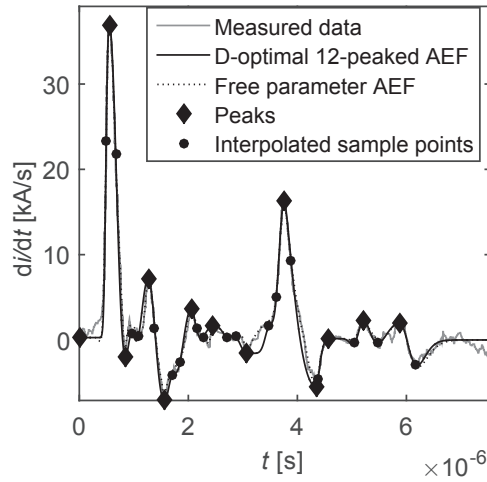


**Fig. 8:** Comparison of two AEFs with 12 peaks and 2 terms in each linear combination fitted to measured lightning discharge current derivative from [20]. One is fitted by interpolation on  $D$ -optimal points and one is fitted with free parameters using the MLSM method. Parameters are given in Table 7.

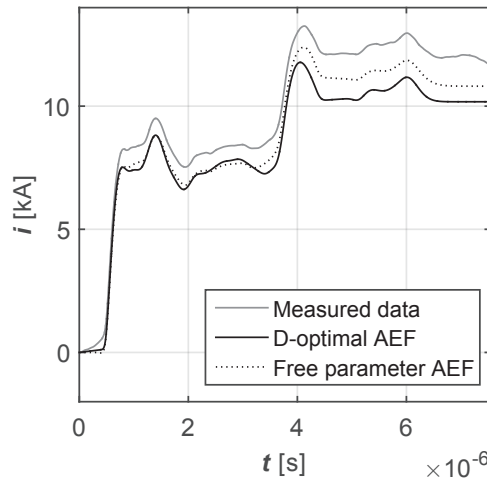


**Fig. 9:** Comparison of results of integrating the results shown in fig. 8.

**Table 7:** Parameters' value of AEF with 12 peaks representing measured data for a lightning discharge current derivative from [20]. Chosen peak times are denoted  $t$  and  $I$  and other parameters correspond to the fitted AEF shown in fig. 8.

Peak times and currents		Parameters of fitted AEF			
$t$ [ $\mu\text{s}$ ]	$I$ [ $\mu\text{s}$ ]	Interval	$n$	$k$	$c$
$t_0 = -0.3437$	$I_0 = 0$	$t_0 \leq t \leq t_1$	2	10	0.06099
$t_1 = 0.9468$	$I_1 = 36.65$	$t_1 \leq t \leq t_2$	2	1	0.4506
$t_2 = 0.5001$	$I_2 = -2.208$	$t_2 \leq t \leq t_3$	3	1	0.04772
$t_3 = 0.9215$	$I_3 = 6.89$	$t_3 \leq t \leq t_4$	2	1	0.4502
$t_4 = 1.212$	$I_4 = -7.322$	$t_4 \leq t \leq t_5$	3	1	0.2590
$t_5 = 1.714$	$I_5 = 3.402$	$t_5 \leq t \leq t_6$	3	2	0.9067
$t_6 = 2.103$	$I_6 = 1.319$	$t_6 \leq t \leq t_7$	3	1	0.3333
$t_7 = 2.730$	$I_7 = -1.844$	$t_7 \leq t \leq t_8$	3	1	0.03732
$t_8 = 3.416$	$I_8 = 16.08$	$t_8 \leq t \leq t_9$	2	4	3.3793
$t_9 = 4.005$	$I_9 = -5.787$	$t_9 \leq t \leq t_{10}$	2	1	1.4912
$t_{10} = 4.216$	$I_{10} = -0.1268$	$t_{10} \leq t \leq t_{11}$	2	2	0.09448
$t_{11} = 4.875$	$I_{11} = 1.972$	$t_{11} \leq t \leq t_{12}$	2	6	2.288
$t_{12} = 5.538$	$I_{12} = 1.683$	$t_{13} < t$	3	1	0.001705

## 5 CONCLUSION

In this work we examine a mathematical model for representation of various ESD currents or their derivative and apply it to some realistic cases, either taken from standards, see section 4.1.1 and 4.2.1, or measured data, see sections 4.1.2, 4.2.2 and 4.2.3.

The model is based around the multi-peaked analytically extended function (AEF), see section 2.1, has been proposed and successfully applied to lightning current modelling in [6, 9–11].

It matches common requirements of ESD-type currents, such as stating that the function and its first derivative must be equal to zero at the starting time. Furthermore, the AEF function is time-integrable, [11], which is necessary for numerical calculation of radiated fields originating from the ESD current.

We construct the model by restricting the exponents in the AEF to an arithmetic sequence and then interpolate points of the function we wish to approximate chosen according to a  $D$ -optimal design. This makes the modelling less flexible than the case where all exponents can be chosen freely but gives a scheme for fitting the function that scales better to many data points than the MLSM fitting scheme used in [6, 9–11].

The resulting methodology can give fairly accurate results even with a modest number of interpolated points but strategies for choosing some of the involved parameters should be further investigated. The decaying part of the waveforms are consistently difficult to fit and if the models are used in a context where significant error propagation appears a more flexible approach can be desirable.

## ACKNOWLEDGMENTS

The authors would like to thank Dr. Pavlos Katsivelis from the High Voltage Laboratory, School of Electrical and Computer Engineering, National Technical University of Athens, Greece, for providing measured ESD current data.

## REFERENCES

- [1] K. Lundengård, M. Rančić, V. Javor, and S. Silvestrov, "Multi-Peaked Analytically Extended Function Representing Electrostatic Discharge (ESD) Currents," in *AIP Conference Proceedings ICNPAA, La Rochelle, France*, pp. 1–10, 2016.

- [2] V. Javor, "Multi-Peaked Functions for Representation of Lightning Channel-Base Currents," 31st Int. Conference on Lightning Protection ICLP 2012, September 2-7, 2012, Proceedings of papers, Vienna, Austria, 2012.
- [3] V. Javor, "New function for representing IEC 61000-4-2 standard electrostatic discharge current," *Facta Universitatis, Series: Electronics and Energetics*, vol. 27(4), pp. 509–520, 2014.
- [4] V. Javor, K. Lundengård, M. Rančić, and S. Silvestrov, "Measured electrostatic discharge currents modeling and simulation," in *Proc. of TELSIKS 2015, Niš, Serbia*, pp. 209–212, 2015.
- [5] V. Javor, "New Function for Representing IEC 61000-4-2 Standard Electrostatic Discharge Current," (invited paper), *Facta Universitatis, Series Electronics and Energetics*, Vol. 27(4), pp. 509–520, University of Ni, Serbia, 2014.
- [6] V. Javor, K. Lundengård, M. Rancic, S. Silvestrov, "Analytical Representation of Measured Lightning Currents and Its Application to Electromagnetic Field Estimation," *IEEE Transactions on Electromagnetic Compatibility*, vol. 60(5), pp. 1415–1426, 2018.
- [7] K. Lundengård, M. Rančić, V. Javor, and S. Silvestrov, "Application of the Marquardt least-squares method to the estimation of Pulse function parameters," in *AIP Conference Proceedings 1637, ICNPAA, Narvik, Norway*, 2014, pp. 637–646.
- [8] K. Lundengård, M. Rančić, V. Javor, and S. Silvestrov, "Estimation of Pulse function parameters for approximating measured lightning currents using the Marquardt least-squares method," in *Conference Proceedings, EMC Europe, Gothenburg, Sweden*, 2014, pp. 571–576.
- [9] K. Lundengård, M. Rančić, V. Javor, and S. Silvestrov, "An Examination of the multi-peaked analytically extended function for approximation of lightning channel-base currents," in *Proceedings of Full Papers, PES 2015, Niš, Serbia*, Electronic, arXiv:1604.06517 [physics.comp-ph], 2015.
- [10] K. Lundengård, M. Rančić, V. Javor, and S. Silvestrov, "Application of the multi-peaked analytically extended function to representation of some measured lightning currents," *Serbian Journal of Electrical Engineering*, vol. 13(2), pp. 1–11, 2016.
- [11] K. Lundengård, M. Rančić, V. Javor, and S. Silvestrov, "Estimation of parameters for the multi-peaked AEF current functions," *Methodol. Comp. Appl. Probab.*, pp. 1–15, 2016.
- [12] K. Lundengård, M. Rančić, V. Javor, and S. Silvestrov, "On some properties of the multi-peaked analytically extended function for approximation of lightning discharge currents" in: Sergei Silvestrov and Milica Rančić, editors, *Engineering Mathematics I: Electromagnetics, Fluid Mechanics, Material Physics and Financial Engineering*, volume 178 of *Springer Proceedings in Mathematics & Statistics*. Springer International Publishing, 2016.

- [13] K. Lundengård, M. Rančić, V. Javor, and S. Silvestrov, "Novel Approach to Modelling of Lightning Current Derivative," *Facta Universitatis, Series Electromagnetics and Energetics*, vol. 30(2), pp. 245–256, University of Ni, Serbia 2017.
- [14] EMC - Part 4-2: Testing and Measurement Techniques - Electrostatic Discharge Immunity Test. IEC International Standard 61000-4-2, basic EMC publication, 1995+A1:1998+A2:2000.
- [15] EMC - Part 4-2: Testing and Measurement Techniques - Electrostatic Discharge Immunity Test. IEC International Standard 61000-4-2, basic EMC publication, Ed. 2, 2009.
- [16] P. S. Katsivelis, I. F. Gonos, and I. A. Stathopoulos, "Estimation of parameters for the electrostatic discharge current equation with real human discharge events reference using genetic algorithms," *Meas. Sci. Technol.*, vol. 21, pp. 1–6, 2010.
- [17] Protection against lightning electromagnetic impulse - Electrostatic Discharge Immunity Test. IEC International Standard 61312-1, 1995.
- [18] F. Heidler and J. Cvetić, "A Class of Analytical Functions to Study the Lightning Effects Associated With the Current Front," *ETEP*, vol. 12(2), pp. 141–150, 2002.
- [19] F. Delfino, R. Procopio, M. Rossi, F. Rachidi, "Prony Series Representation for the Lightning Channel Base Current," *IEEE Transactions on Electromagnetic Compatibility*, vol. 54(2), pp. 308–315, 2012.
- [20] A. Hussein, M. Milewski, W. Janischewskyj, "Correlating the Characteristics of the CN Tower Lightning Return-Stroke Current with Those of Its Generated Electromagnetic Pulse," *IEEE Transactions on Electromagnetic Compatibility*, vol. 50(3), pp. 642–650, 2008.
- [21] G. P. Fotis, and L. Ekonomu, "Parameters' optimization of the electrostatic discharge current equation," *Int. journal on Power System Optimization*, vol. 3(2), pp. 75–80, 2011.
- [22] V. B. Melas, *Functional Approach to Optimal Experimental Design*. New York: Springer, 2006.
- [23] M. Abramowitz and I. Stegun, *Handbook of Mathematical Functions with Formulas, Graphs, and Mathematical Tables*. New York: Dover, 1964.
- [24] T. S. Chihara, *An Introduction to Orthogonal Polynomials*. Gordon and Breach, Science Publishers, Inc., New York, 1978.
- [25] K. Driver and K. Jordaan, "Bounds for extreme zeros of some classical orthogonal polynomials", *J. Approx. Theory* 164(9), pp. 1200–1204, 2012.
- [26] F. R. Lucas, "Limits for zeros of Jacobi and Laguerre polynomials", *Proceeding Series of the Brazilian Society of Applied and Computational Mathematics* 3(1), 2015.
- [27] MATLAB and Optimization Toolbox Release 2015a, function `lsqnonlin`, The MathWorks, Inc., Natick, Massachusetts, United States.

- [28] T.F. Coleman and Y. Li. "On the Convergence of Reflective Newton Methods for Large-Scale Nonlinear Minimization Subject to Bounds.", *Mathematical Programming* 67(2), pp. 189-224, 1994.
- [29] T.F. Coleman and Y. Li. "An Interior, Trust Region Approach for Nonlinear Minimization Subject to Bounds.", *SIAM Journal on Optimization*, Vol. 6, pp. 418-445, 1996.
- [30] A. Rubinstein, C. Romero, M. Paolone, F. Rachidi, M. Rubinstein, P. Zweiacker, and B. Daout, Lightning measurement station on Mount Säntis in Switzerland, in *Proc. Xth Int. Symp. Lightning Protection*, Curitiba, Brazil, pp. 463-468, 2009.